Drug and Chemical Toxicology

ISSN: 0148-0545 (Print) 1525-6014 (Online) Journal homepage: www.tandfonline.com/journals/idct20

Computational investigation of m-acetamide and 3MPAEA: Characterization, toxicity, and molecular docking and dynamic analyses

Nevin Çankaya, Mehmet Hanifi Kebiroğlu & Serap Yalcin Azarkan

To cite this article: Nevin Çankaya, Mehmet Hanifi Kebiroğlu & Serap Yalcin Azarkan (2025) Computational investigation of m-acetamide and 3MPAEA: Characterization, toxicity, and molecular docking and dynamic analyses, Drug and Chemical Toxicology, 48:5, 943-958, DOI: 10.1080/01480545.2025.2496358

To link to this article: https://doi.org/10.1080/01480545.2025.2496358

DRUG AND CHEMICAL TOXICOLOGY
2025, VOL. 48, NO. 5, 943–958
https://doi.org/10.1080/01480545.2025.2496358

Taylor & Francis
Taylor & Francis Group

RESEARCH ARTICLE

Computational investigation of m-acetamide and 3MPAEA: Characterization, toxicity, and molecular docking and dynamic analyses

Nevin Çankaya[a], Mehmet Hanifi Kebiroğlu[b] and Serap Yalcin Azarkan[c]

[a]Vocational School of Health Services, Usak University, Usak, Turkey; [b]Darende Bekir Ilicak Vocational School, Department of Opticianry, Malatya Turgut Ozal University, Malatya, Turkey; [c]Department of Medical Pharmacology, Faculty of Medicine, Kırsehir Ahi Evran University, Kırşehir, Turkey

ABSTRACT

In this study, 2-(3-methoxyphenylamino)-2-oxoethyl acrylate (3MPAEA) molecule was synthesized in two steps. In the first step, 2-chloro-N-(3-methoxyphenyl)acetamide (m-acetamide) was obtained. Density functional theory (DFT) calculations were performed to obtain information about the electronic and structural properties of the synthesized molecules. The Raman Spectrum and UV-Visible analysis were calculated using the Gaussian package program. Additionally, Natural Bond Orbital (NBO) Analysis, Electron Localization Function (ELF), Electrostatic Potential Map (ESP), Average Local Ionization Energy (ALIE), and the toxicological properties of the molecules were examined. Simultaneously, molecular docking and dynamic analyses were conducted to investigate the interaction of m-acetamide and 3MPAEA with proteins involved in nuclear receptor signaling pathways, stress response pathways, molecular initiating events, and metabolism, as identified in the protox analysis. The findings aligned with the protox analysis results. The results obtained provide new insights into the electronic and toxicological properties of these molecules.

ARTICLE HISTORY
Received 28 January 2025
Revised 27 March 2025
Accepted 16 April 2025

KEYWORDS
DFT; NBO; ESP; ALIE; in silico toxicology; molecular docking; molecular dynamic

1. Introduction

Acrylates, as versatile organic compounds, play a critical role in fields like polymer chemistry, material science, and the pharmaceutical industry (Alhewaitey et al., 2024). Their ability to undergo polymerization and form complex structures makes them indispensable in the development of adhesives, coatings, plastics, and biomedical devices (Yadav et al., 2024). Among acrylate derivatives, those functionalized with aromatic amine groups are intriguing due to their enhanced reactivity and tunable electronic properties. Introducing substituents on the phenyl ring, such as methoxy groups, can influence the electron distribution in these molecules, altering their stability, reactivity, and interactions with other compounds (Zucolotto Cocca et al., 2024). The compound 2–(3-methoxyphenylamino)-2-oxoethyl acrylate (3MPAEA) represents a novel derivative within this family of functionalized acrylates. The 3-methoxyphenylamino group present in the molecular structure provides both electron-donating and resonance effects, which can significantly influence its chemical behavior (Zhou et al., 2020). This structural motif is important not only for adjusting the electronic properties but also for introducing potential interactions with biological systems (Patil et al., 2024). This makes 3MPAEA a compound of interest in fields such as drug development, photochemistry, and material science. The electron-donating effect of the methoxy group can alter the conjugation and electronic distribution, thus affecting the molecule's optical and spectroscopic properties (Qiao et al., 2024). Although acrylates have been extensively studied, research on the spectroscopic and electronic characteristics of 3MPAEA and its derivatives is limited (Çankaya et al., 2024). In this study, synthesizes 3MPAEA by a two-step process and analyzes its molecular properties. In the first step of the synthesis, 2-chloro-N-(3-methoxyphenyl)acetamide (m-acetamide), an important intermediate in the formation of 3MPAEA, was prepared. The reaction sequence was carefully designed to preserve the functional groups and ensure the successful introduction of the acrylate moiety. After the synthesis of 3MPAEA, a comprehensive analysis of its spectroscopic and electronic properties was conducted. These analyses are crucial for identifying the reactive regions within the molecule and understanding how it may interact with other chemical species (Zhang et al., 2024). To investigate the *in silico* biological and toxic properties of both molecules, ProTox 3.0 (https://tox.charite.de/protox3/) program was used and molecular docking analyses were performed according to the results obtained from ProTox. ProTox 3.0 is a virtual toxicity laboratory developed for academic and non-commercial users, analyzing multiple endpoints to predict the toxicological effects of chemical structures (Jurowski & Krośniak, 2024). Docking calculations were performed using AutoDock Vina, and the resulting interactions, including hydrogen (H)-bonds, were visualized using the Seamdock

CONTACT Nevin Çankaya nevin.cankaya@usak.edu.tr, nevincankaya@hotmail.com Vocational School of Health Services, Usak University, Usak 64200, Turkey

online tool (https://bioserv.rpbs.univ-paris-diderot.fr/services/SeamDock/) (Çoban et al., 2024). Then, molecular dynamics analysis was performed to determine the stability of the binding of molecules with proteins with binding energy above −6.5 kcal/mol. Toxicological predictions were made to assess the environmental and biological safety of m-acetamide and 3MPAEA, and these results were confirmed by molecular docking and dynamic analyses, providing valuable information for its potential applications in pharmaceutical and industrial fields (Çankaya et al., 2024).

2. Methods

2.1. Experimental methods

The synthesis of 2–(3-methoxyphenylamino)-2-oxoethyl acrylate (3MPAEA) was conducted using a two-step approach. In the initial step, 2-chloro-N-(3-methoxyphenyl)acetamide (m-acetamide) was prepared via the reaction of 3-methoxyaniline with chloroacetyl chloride under controlled conditions (Çoban et al., 2024). In the second step, 3MPAEA was prepared by the reaction of m-acetamide with sodium acrylate (Çankaya et al., 2024). Figure 1 illustrates the chemical structures of m-acetamide and 3MPAEA.

2.2. Quantum chemical calculations

To investigate the vibrational characteristics of 3MPAEA, Raman spectroscopy was utilized. UV-Visible spectroscopy was employed to analyze the electronic transitions of 3MPAEA in various solvents (Arulaabaranam et al., 2021). To gain further insights into the electronic and structural properties of both m-acetamide and 3MPAEA, density functional theory (DFT) calculations were performed. DFT/B3LYP/6-311G, this basis set was used to achieve highly accurate predictions of molecular geometry, electron distribution, and vibrational frequencies for both m-acetamide and 3MPAEA. DFT/B3LYP/LanL2DZ, this basis set was applied to systems involving heavier atoms to balance computational cost and accuracy, particularly for 3MPAEA (Çankaya et al., 2024).

The computational approach utilized in this study aligns well with methodologies reported in previous DFT studies on organic derivatives. For instance Medimagh et al., successfully applied B3LYP calculations with the CC-PVTZ basis set to investigate structural, electronic, and vibrational properties of organic-inorganic hybrid compounds. Their findings emphasized the significance of accurately modeling non-covalent interactions and electron delocalization for predicting molecular stability and properties (Medimagh et al., 2021). Therefore, the computational strategy adopted here is validated by similar studies, reinforcing its suitability and reliability for analyzing the molecules examined in our research.

To strengthen the motivation of this study, comparisons have been made with previous computational studies on similar acrylate derivatives to demonstrate the accuracy and suitability of the methods used for geometry optimization and determining electronic properties (Gatfaoui et al., 2019). For example Gatfaoui et al., successfully modeled molecular structures and electronic distributions of various organic compounds using the B3LYP/6-311++G(d,p) method, highlighting the significance of electron delocalization on the electronic properties of materials (Gatfaoui et al., 2022). These comparisons indicate that the theoretical approaches employed for the molecules in the current study follow computational methods widely accepted in the literature for similar structures. The optimization results provide a strong foundation for further analyses, such as electronic structure and bonding interactions (Reeda et al., 2024). To gain deeper insight into the electron distribution and bonding characteristics of these molecules, Natural Bond Orbital (NBO) Analysis was conducted (Halim et al., 2024). NBO calculations allowed for the identification of key donor-acceptor interactions and electron delocalization within the molecular framework (Abdelaziz et al., 2024). Raman spectroscopy is a powerful technique for investigating the vibrational properties of molecules, providing valuable insights into molecular structure and bonding (Boehmke Amoruso et al., 2024).

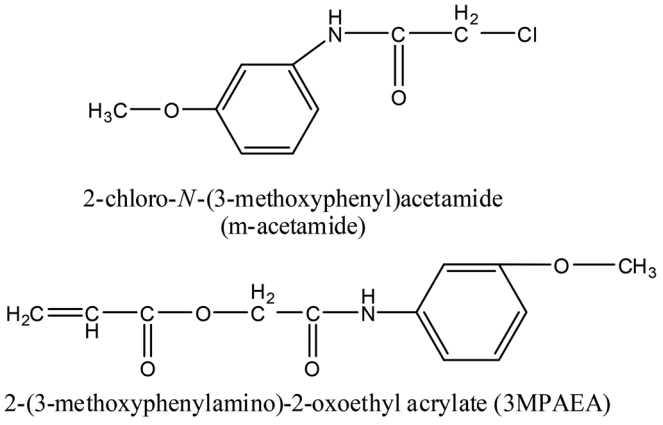

Figure 1. The scheme of m-acetamide and 3MPAEA.

2.3. Atomic and molecular electronic properties

The Electron Localization Function (ELF) is a robust computational method employed to examine the electron distribution within molecules, with a particular emphasis on identifying regions where electrons are highly localized (Ylivainio, 2024). Introduced by Becke and Edgecombe in 1990, ELF visually represents electron density in molecular systems, offering critical insights into bonding interactions, lone pairs, and areas of electron delocalization (Vidal et al., 2024). The total Electrostatic Potential Map (ESP) is a fundamental property used to understand the charge distribution within a molecule and how this affects its interactions with other molecules, particularly in chemical reactivity, molecular recognition, and non-covalent interactions such as hydrogen bonding (Manogaran et al., 2024). The ESP is visualized on the molecular surface with color gradients, where red regions correspond to areas of higher positive potential, and blue regions represent areas of higher negative potential (Boittier et al., 2024). The color bars on the sides provide a quantitative scale of the potential values in Bohr units. This analysis aids in understanding the electrostatic properties of the molecules

and identifying potential interaction sites (GP et al. 2024). Average Local Ionization Energy (ALIE) is a quantum chemical property that indicates the likelihood of electrons being ionized from specific regions of a molecule (Akman, 2025). It is mapped onto the molecular surface, with a color scale on the right showing different ionization energy values. In ALIE's figures, red areas represent regions of higher ionization energy, where electrons are more tightly bound and harder to ionize, while blue areas indicate lower ionization energy, where electrons are more easily ionized.

2.4. In silico toxicity investigation

ProTox 3.0 is an advanced computational model developed for predicting the toxicity of chemicals (Banerjee et al., 2024). Utilizing the ProTox 3.0 model, predictions were made for various toxicity endpoints, organ toxicity, and nuclear receptor signaling pathways, among others (Jurowski et al., 2025). This tool is part of the broader ProTox series, which utilizes machine learning and cheminformatics approaches to predict various toxicological endpoints, such as LD50, ED50, hepatotoxicity, and immunotoxicity (Habiballah et al., 2024). ProTox 3.0 provides detailed insights into the toxicity of chemical compounds based on specific structural descriptors (e.g., electrophilic groups, reactive functional groups, and hydrophobic regions) and their potential interactions with biological systems (Azzouzi et al., 2024). Due to these features, ProTox 3.0 is valuable in drug development, environmental risk assessment, and chemical safety evaluations (Sturla et al., 2014). In this study, the *in silico* toxicity of m-acetamide and 3MPAEA molecules was evaluated using the web-based ProTox 3.0 platform (https://tox.charite.de/protox3/index.php?site=home), predicting toxicity endpoints such as LD50, hepatotoxicity, and mutagenicity.

This study investigates several additional toxicological endpoints and mechanisms, including molecular initiating events (MIEs), metabolic interactions involving cytochrome P450 (CYP450) enzymes, immunotoxicity, ecotoxicity, carcinogenicity, mutagenicity, oxidative stress pathways, stress response signaling pathways, endocrine disruption potential, and Absorption, Distribution, Metabolism, Excretion, and Toxicity (ADMET) profiles (Rifa et al., 2025).

2.5. Molecular docking and dynamic analyses

In the molecular docking and dynamic analysis, we aimed to determine whether m-acetamide and 3MPAEA have inhibitory activity because of docking with the proteins identified in the protox analysis. We explored the potential binding between the molecules and targets using molecular docking techniques. AutoDock Vina (Trott & Olson, 2010) was used for the docking process and the Seamdock online tool (Murail et al., 2021; Yalçınkaya et al., 2022). The pdb files of key genes were retrieved from PDB, followed by docking with AutoDock Vina. PDB ID codes are given in the Table 1. In this study, ADME analyses of molecules were analyzed with Protox 3.0. The three-dimensional structures of the proteins were obtained in PDB file format from the RCSB PDB database (https://www.rcsb.org/). Docking calculations were carried out using AutoDock (Vina Trott & Olson, 2010), and the resulting interactions, including hydrogen (H)-bonds, were visualized through the Seamdock online tool (Murail et al., 2021). Molecular dynamics simulations for both the proteins and protein-ligand complexes were performed using WebGro, with the stability of unbound and ligand-bound proteins analyzed graphically over a 50-nanosecond (ns) simulation period (Abraham et al., 2015; Bjelkmar et al., 2010; Lindorff-Larsen et al., 2010; Oostenbrink et al., 2004; Yalçınkaya et al., 2022). In molecular dynamics analysis, Root means square deviation (RMSD) plots, which measure the stability of a complex structure over time, and Hydrogen bond plots were obtained.

Table 1. Binding position and number of hydrogen bonds of MPAEA and m-acetamide with CYP3A4.

m-acetamide				
Proteins and PDB ID code	Binding energy (kcal/mol)	Hydrogen bond number		Binding position
Cytochrome CYP3A4 (1TQN)	−6.1	Ligand atom	Receptor F108(A) O	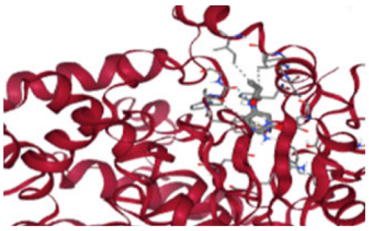
3MPAEA				
Proteins and PDB ID	**Binding energy (kcal/mol)**	**Hydrogen bond number**		**Binding position**
Cytochrome CYP3A4 (1TQN)	−6.9	Ligand atom	Receptor F108(A) O	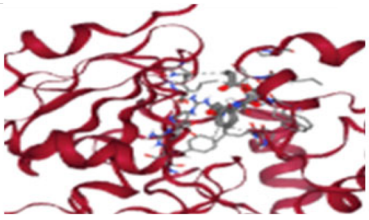
		OG1	NaN() O	

3. Result and discussion

3.1. Geometry optimization and natural bond orbital (NBO) analysis

The geometry optimization of both the m-acetamide and 3MPAEA molecules was performed using density functional theory (DFT) at the B3LYP level with the 6-311 G and LanL2DZ basis sets (Çankaya et al., 2024). These basis sets were selected due to their proven effectiveness in accurately modeling molecular geometries and electronic structures of similar organic compounds; however, comparisons with alternative basis sets such as 6-311++G(d,p) and cc-pVDZ from relevant literature suggest they provide comparable results with slight variations in accuracy depending on the molecule studied (Gatfaoui et al., 2022; Medimagh et al., 2021). In Figure 2, the bond lengths are shown in a color-coded range, with m-acetamide displaying bond lengths from 1.011 to 1.811 Å, and 3MPAEA showing a range of 1.241 to 1.813 Å. These variations in bond length correspond to the different bonds present, including C-H, C-C, C-N, and C=O, and reflect typical bonding behavior in organic molecules. In the 3MPAEA molecule, a highly delocalized electron distribution across the conjugated π-system of the acrylate moiety was observed. Such electronic delocalization follows findings from other DFT studies, which emphasize the importance of accurately describing electron delocalization to understand the electronic and optical properties of organic molecules (Ramalingam et al., 2022). This delocalization contributes to the molecule's electronic properties and is key to understanding its UV-Visible absorption characteristics and overall molecular stability (Joseph et al., 2024). The NBO analysis further supports the findings from geometry optimization, indicating a well-stabilized structure with significant electron delocalization, which is critical for its potential applications in material science and photonic devices (Salah et al., 2023).

3.2. Spectroscopic analyses

The Raman spectra of m-acetamide and 3MPAEA reveal characteristic bands that exhibit both similarities and distinctions. Table 2 shows the assignments of the Raman activities for these two molecules, with particular attention given to the vibrational modes of bonds such as C-H, C=O, and C=C. Figure 3 presents a comparative display of the Raman activities of both molecules, clearly distinguishing the vibrational modes. Similarly, the Raman intensity spectra of both molecules have been analyzed. Table 3 lists the assignments of the main vibrational modes observed in the spectra regarding their intensity. Figure 4 graphically presents these intensities, with both molecules showing strong peaks in the low-frequency region. UV-Visible analysis is a spectroscopic technique that utilizes light in the ultraviolet (UV) and visible (Vis) ranges to investigate the electronic structure and properties of molecules (Ak & Kebiroglu, 2024). By measuring the absorption of light at different wavelengths, this technique provides insights into the electronic transitions within a molecule, including π-π* and n-π* transitions (Abdelaziz et al., 2024). Stabilization energies for donor-acceptor interactions, particularly between oxygen lone pairs and the π* orbitals of adjacent C=O bonds, ranged from 5 to 15 kcal/mol, demonstrating strong resonance effects (Nikrou Siahsary et al., 2024). These transitions are typically observed in the UV-Visible region, making this analysis essential for understanding

Table 2. Assignment of Raman activity of m-acetamide and 3MPAEA.

Vibrational Mode	Frequency (cm^{-1})	m-acetamide	3MPAEA	Assignment
C-H Stretching (Aromatic/ Alkyl)	3000–3500	Strong	Strong	C-H bond vibrations in both aromatic and alkyl groups
C=O Stretching (Acrylate)	1650–1750	Weak/Absent	Strong	Stretching of the carbonyl group (only in 3MPAEA)
C=C Stretching (Acrylate)	1600–1700	Absent	Moderate	Double bond stretching in the acrylate moiety (3MPAEA)
Amide Stretching (N-H)	3300–3500	Strong	Moderate	N-H stretching vibrations, predominant in m-acetamide
C-N Stretching	1200–1500	Moderate	Moderate	C-N bond vibrations in both molecules
Aromatic Ring Stretching	500–1500	Moderate	Weak/ Moderate	Vibrational modes related to the phenyl group

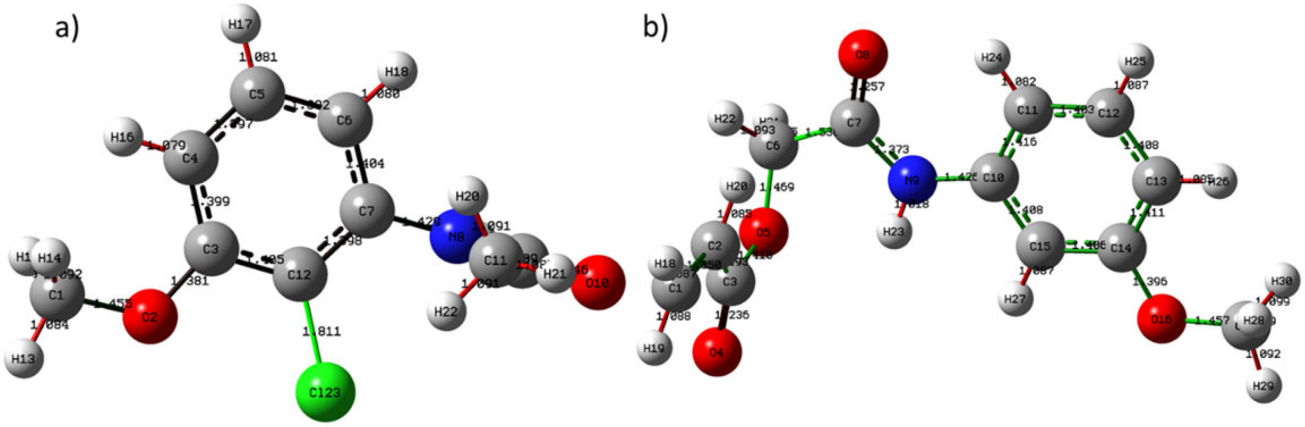

Figure 2. Bond lengths color range of a) 1.011 to 1.811, b) 1.241 to 1.813.

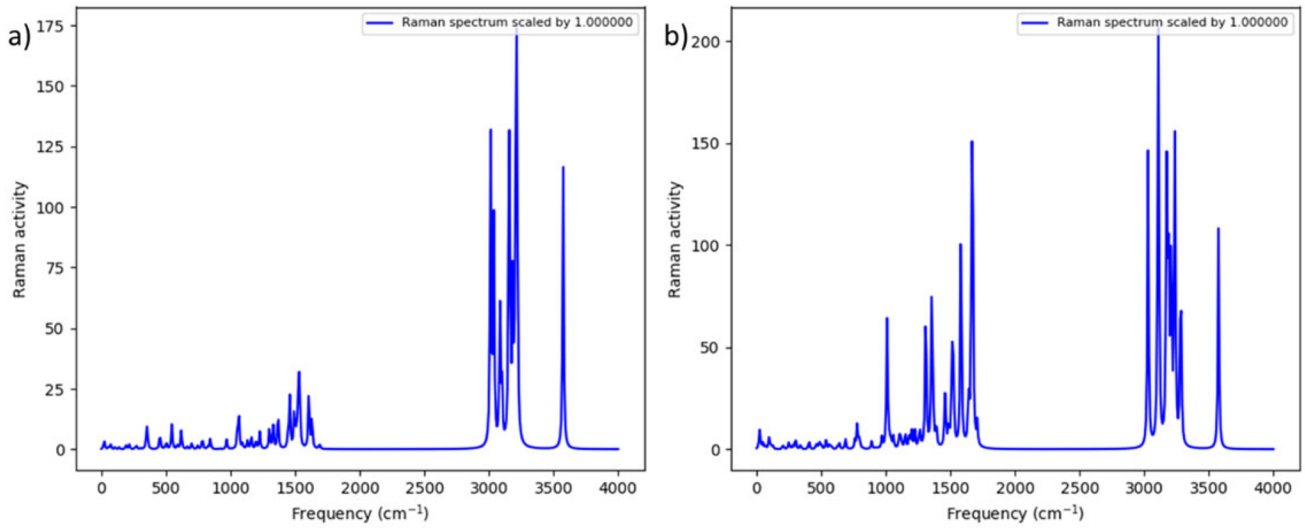

Figure 3. Raman activity of a) m-acetamide, b) 3MPAEA.

Table 3. Assignment of Raman intensity of m-acetamide and 3MPAEA.

Vibrational Mode	Frequency (cm^{-1})	m-acetamide	3MPAEA	Assignment
Low-Frequency Vibrations (Torsional/ Bending)	0–500	Very High	Very High	Strong low-frequency vibrations, likely torsional and bending modes
C-H Stretching (Aromatic/ Alkyl)	3000–3500	Low	Low	C-H bond vibrations in both aromatic and alkyl groups
C=O Stretching (Acrylate)	1650–1750	Absent	Moderate	Stretching of the carbonyl group (only in 3MPAEA)
C=C Stretching (Acrylate)	1600–1700	Absent	Moderate	Double bond stretching in the acrylate moiety (3MPAEA)
Amide Stretching (N-H)	3300–3500	Moderate	Low	N-H stretching vibrations, predominant in m-acetamide

molecular behavior under various energy conditions. Table 4 summarizes the UV-Visible absorption characteristics for the first molecule. Spectral changes were observed by varying the parameter number of excited states (N), beginning with $N=6$ and increasing to 12, 32, and 64, allowing for an exploration of the molecule's photonic behavior (Hyun & Kim, 2024). The absorption maxima shift across a range of wavelengths as the oscillator strength values ($N=6$, 12, 32, 64) increase, indicating changes in electronic transitions as shown in Figure 5. In the UV analysis, different N values (6, 12, 32, and 64) represent varying numbers of excited states in the calculation, significantly affecting spectral properties. Lower N values (e.g., 6 or 12) typically provide basic spectral features but may omit higher-energy transitions, while higher N values (e.g., 32 or 64) can capture a more detailed and comprehensive spectral profile, including weaker transitions and finer details of electronic absorption. This method of varying N is crucial for balancing computational efficiency with accuracy and completeness of spectral information (Akman et al., 2023; Ghalla et al., 2014). These transitions are concentrated primarily in the 200–280 nm range, with distinct peaks representing various molecular interactions. Similarly, the second molecule's UV-Visible absorption features are outlined in Table 5, which highlights the more complex absorption pattern due to additional functional groups. The absorption spectra, depicted in Figure 6, cover a wider wavelength range from 150 to 350 nm, with multiple peaks corresponding to increasing N values. These peaks reflect the enhanced electronic structure and transition density, offering valuable information about the molecule's photophysical properties (Zhao et al., 2024). The theoretical Raman and UV-Visible spectra obtained from the DFT calculations showed good agreement when compared with similar experimental and theoretical studies in the literature, thus validating the accuracy of the results obtained in this study (Ghalla et al., 2014). These optimizations provided the minimum energy configurations and were confirmed to be free of imaginary frequencies through vibrational analysis, ensuring the stability of the optimized structures (Kurban et al., 2024). The resulting bond lengths, bond angles, and dihedral angles are in line with known values for similar acrylate derivatives, validating the accuracy of the computational model (Smati et al., 2024). Significant delocalization was observed between the lone pairs on oxygen atoms and the adjacent nitrogen atoms in both molecules, particularly in the carbonyl groups (Xiong et al., 2024). This delocalization plays a crucial role in stabilizing the molecular structure, as evidenced by second-order perturbation theory calculations (Reeda et al., 2024). The torsional and bending vibrations in the low-frequency range are pronounced for both molecules, manifesting as high-intensity peaks in the spectrum (Obloy et al., 2024).

3.3. Atomic and molecular electronic properties

The electronic properties of the studied molecules were analyzed through ELF, ESP, and ALIE distributions to understand

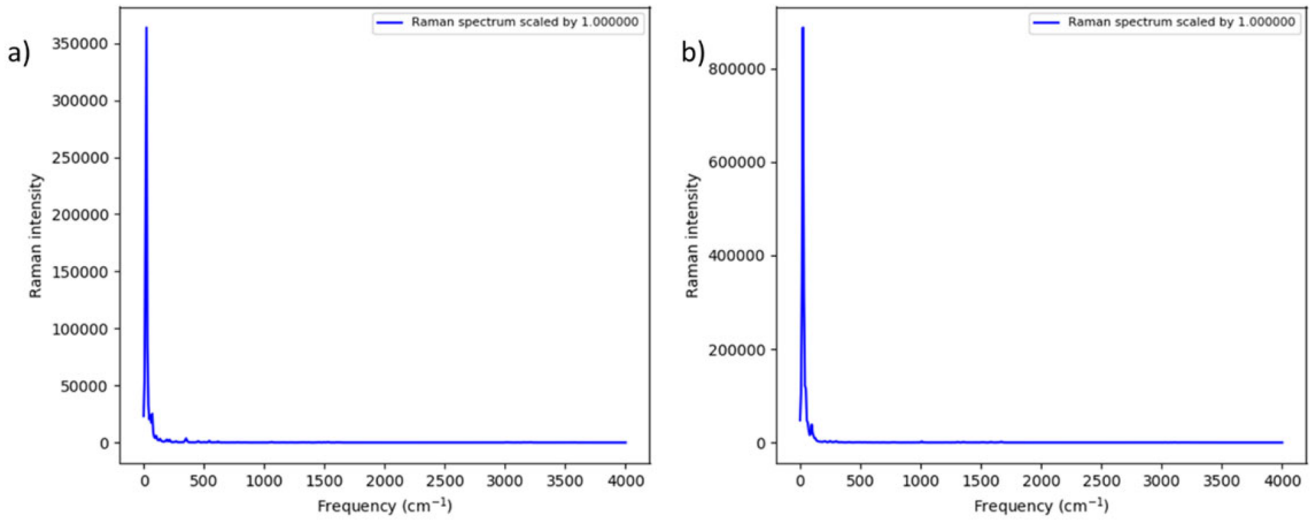

Figure 4. Raman intensity of a) m-acetamide b) 3MPAEA.

Table 4. UV-visible absorption summary for m-acetamide.

N Value	Absorption Maximum (nm)	Oscillator Strength (Range)	Primary Peaks Observed
6	240	0.00 – 0.04	1 peak at 240 nm
12	220	0.00 – 0.175	2 peaks at 200 and 220 nm
32	200	0.00 – 0.225	Multiple peaks from 180-220 nm
64	180	0.00 – 0.25	Multiple peaks from 140-200 nm

the atomic and molecular characteristics of m-acetamide and 3MPAEA. These analyses provided detailed insights into electron localization, electrostatic potential, and ionization energy within the molecular frameworks. The ELF analysis, as visualized in Figure 7, revealed distinct electron localization patterns in m-acetamide and 3MPAEA. In m-acetamide, the localization was concentrated around electronegative atoms, indicating a stronger bonding interaction. The ELF map for 3MPAEA highlighted delocalized electron density in certain regions, which can be attributed to the molecule's unique functional groups. The total electrostatic potential distributions, illustrated in Figure 8, showed significant differences between the two molecules. In m-acetamide, the ESP map demonstrated a higher density around the carbonyl group, consistent with its strong electrophilic nature. Conversely, the ESP distribution for 3MPAEA displayed regions of both positive and negative potentials, indicative of the molecule's bifunctional characteristics. Figure 9 highlights the ALIE distributions for both molecules. For m-acetamide, high ionization energy values were localized near the carbonyl oxygen, reflecting the strong bonding and electron-withdrawing nature of the group. However, 3MPAEA exhibited moderate ionization energies across its structure, corresponding to its relatively balanced electron distribution and reactive sites. These analyses underline the significant differences in the electronic characteristics of m-acetamide and 3MPAEA, influenced by their molecular structure and functional groups. The combined insights from ELF, ESP, and ALIE distributions provide a comprehensive understanding of the electronic behavior of these compounds, aiding in their potential applications in chemical and material sciences.

3.4. Toxicity evaluations

Toxicological assessments of two compounds, m-acetamide and 3MPAEA, were conducted using the ProTox 3.0 model (Drwal et al., 2014). According to ProTox 3.0 analysis, m-acetamide was found to exhibit neurotoxic (probability 0.79) and nephrotoxic (probability 0.55) effects in terms of organ toxicity. The same compound was also identified as active for crossing the blood-brain barrier (probability 0.89), ecotoxicity (probability 0.63), and clinical toxicity (probability 0.63). However, it was assessed as inactive regarding hepatotoxicity, respiratory toxicity, and cardiotoxicity. Additionally, m-acetamide did not show any negative impact in terms of carcinogenicity, immunotoxicity, mutagenicity, cytotoxicity, and nutritional toxicity. Upon examination of nuclear receptor signaling pathways, stress response pathways, molecular initiating events within the Tox21 framework, and cytochrome P450 metabolism, all parameters were determined to be inactive. Regarding the compound 3MPAEA, it was determined to be active only in terms of nephrotoxicity (probability 0.68) within the scope of organ toxicity, while it exhibited no negative effects for other organ toxicities (hepatotoxicity, neurotoxicity, respiratory toxicity, and cardiotoxicity). Additionally, 3MPAEA was identified as active for crossing the blood-brain barrier (probability 0.68) and clinical toxicity (probability 0.64). However, it posed no risk in terms of carcinogenicity, immunotoxicity, mutagenicity, cytotoxicity, ecotoxicity, and nutritional toxicity. The assessment of nuclear receptor signaling pathways, stress response pathways, molecular initiating events within the Tox21 framework, and cytochrome P450 enzymes revealed that the compound did not exhibit any negative effects (Supplementary Material Tables S5 and S6). These results are significant for detailing the toxicological profiles and predicting the potential toxic effects of both compounds (Drwal et al., 2014).

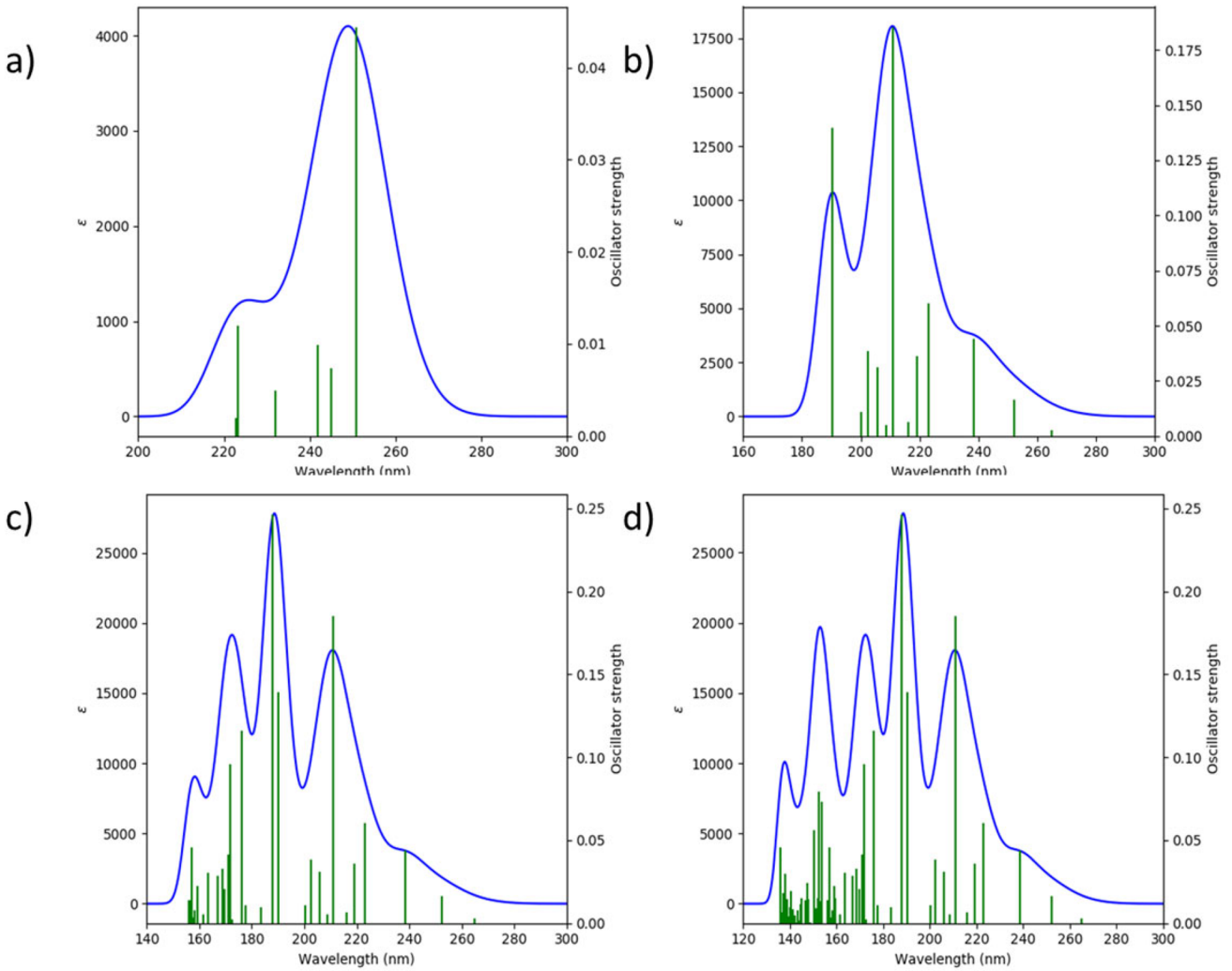

Figure 5. UV-visible (6,12,32,64) absorption of m-acetamide.

Table 5. UV-visible absorption summary for 3MPAEA.

N Value	Absorption Maximum (nm)	Oscillator Strength (Range)	Primary Peaks Observed
6	280	0.00 – 0.04	1 peak at 280 nm
12	250	0.00 – 0.25	Multiple peaks from 200-250 nm
32	200	0.00 – 0.25	Multiple peaks from 180-250 nm
64	180	0.00 – 0.25	Multiple peaks from 150-250 nm

The toxicological predictions for m-acetamide (Supplementary Material Table S5) and 3MPAEA (Supplementary Material Table S6) offer important insights into their potential biological and environmental impacts. For m-acetamide, the prediction results indicate neurotoxicity and nephrotoxicity with probabilities of 0.79 and 0.55, respectively, while other organ toxicities such as hepatotoxicity and cardiotoxicity were predicted as inactive. The ProTox 3.0 platform predicts toxicity outcomes using machine learning algorithms trained on large toxicological datasets (Banerjee et al., 2024). For each outcome, the model outputs a probability score ranging from 0 to 1, reflecting the confidence in assigning the classification as 'Active' or 'Inactive', with implied complementary probability (e.g., P(Active) = 1 – P(Inactive)). Probabilities closer to 0.5 reflect the model's threshold-based decision boundary, indicating lower confidence in prediction. The blood-brain barrier (BBB) penetration for m-acetamide is predicted to be active with a high probability of 0.89, suggesting that the compound may pass into the central nervous system. Additionally, the molecule shows clinical toxicity and ecotoxicity with probabilities of 0.63 each. Clinical toxicity (probability: 0.63) indicates that both compounds (m-acetamide and 3MPAEA) might cause adverse health effects upon exposure, especially related to neurological (central nervous system) or renal (kidney) impairment, warranting further medical or toxicological evaluation. Ecotoxicity (probability: 0.63 for m-acetamide) suggests these compounds may pose environmental hazards, potentially affecting aquatic or terrestrial life if released into ecosystems. This necessitates ecological safety assessments. Thus, clinical toxicity focuses on human or animal health effects, while ecotoxicity focuses on environmental impact and safety.

Regarding molecular initiating events and metabolic interactions, m-acetamide was predicted to be inactive across most pathways, including cytochrome enzymes and nuclear receptor pathways, with high confidence in some cases, such

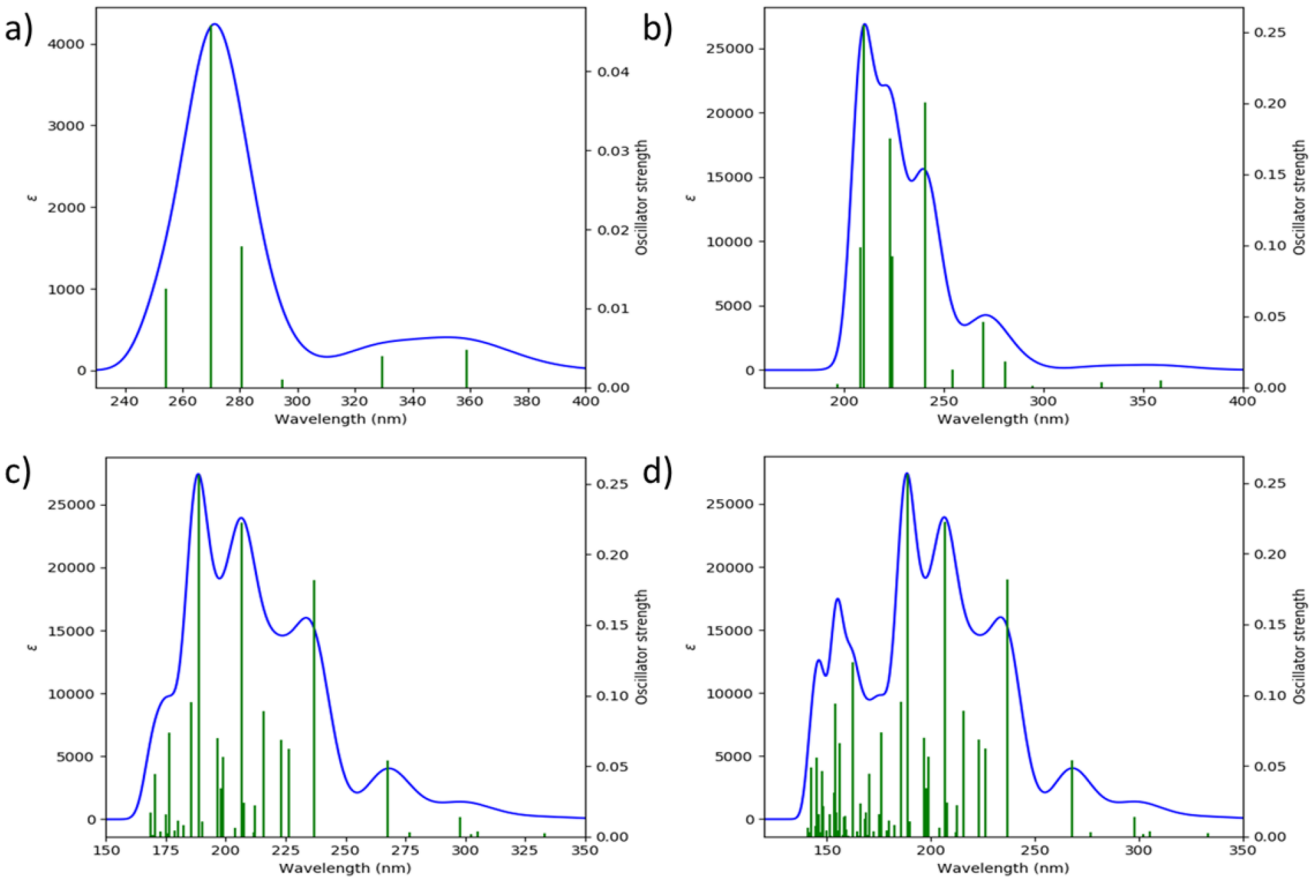

Figure 6. UV-visible (6,12,32,64) absorption of 3MPAEA.

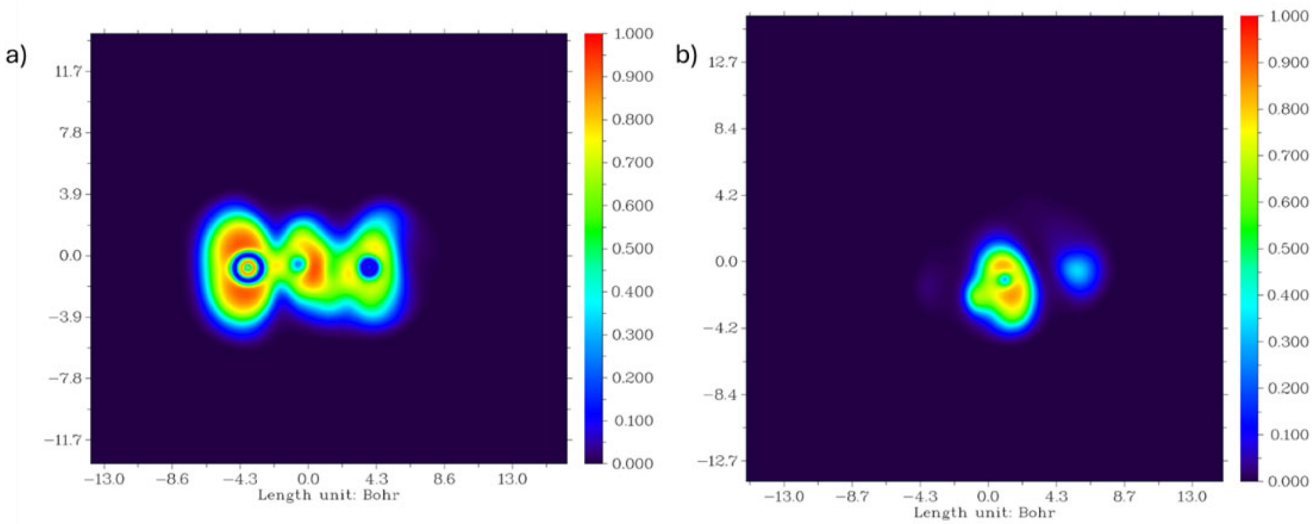

Figure 7. Electron localization function (ELF) for a) m-acetamide b) 3MPAEA.

as for CYP2E1 (0.99) and PPAR-Gamma (0.99). For 3MPAEA, the predictions reveal nephrotoxicity with a probability of 0.68, alongside activity at the BBB (0.68) and clinical toxicity (0.64). Similar to m-acetamide, most other organ toxicity markers, including hepatotoxicity and cardiotoxicity, were predicted as inactive. Immunotoxicity was also inactive with a relatively high probability (0.79).

It is noteworthy that, despite the relatively high probability score of 0.79 associated with Immunotoxicity for 3MPAEA, the outcome was classified as inactive. This apparent contradiction arises from the ProTox 3.0 model, which utilizes a threshold-based classification system. Probabilities above 0.5 typically indicate that the model confidently predicts inactivity, while values significantly below 0.5

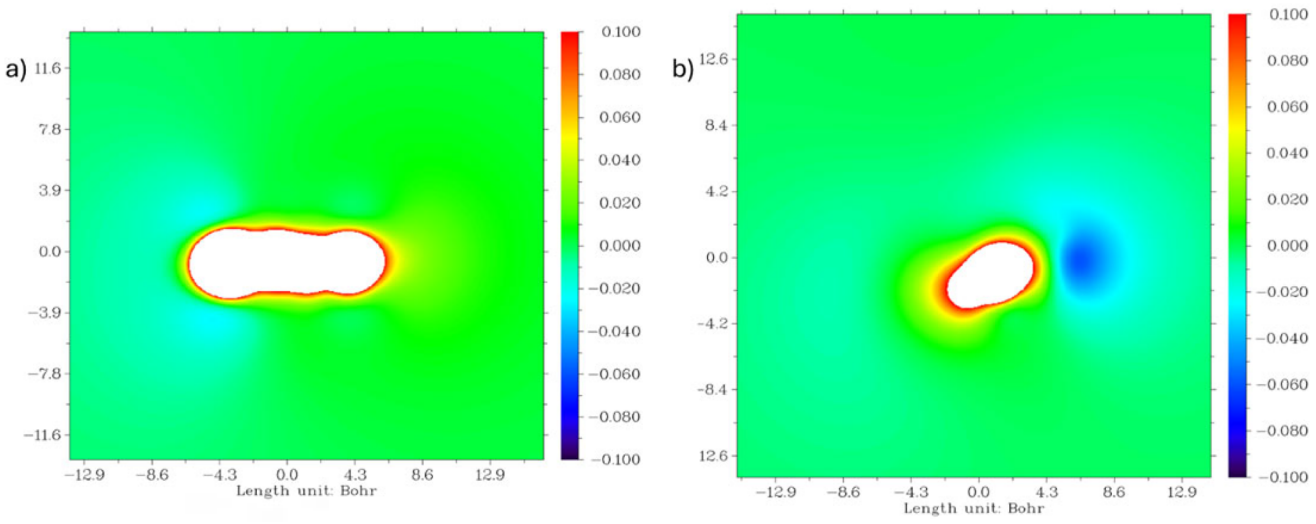

Figure 8. Total electrostatic potential (ESP) for a) m-acetamide b) 3MPAEA.

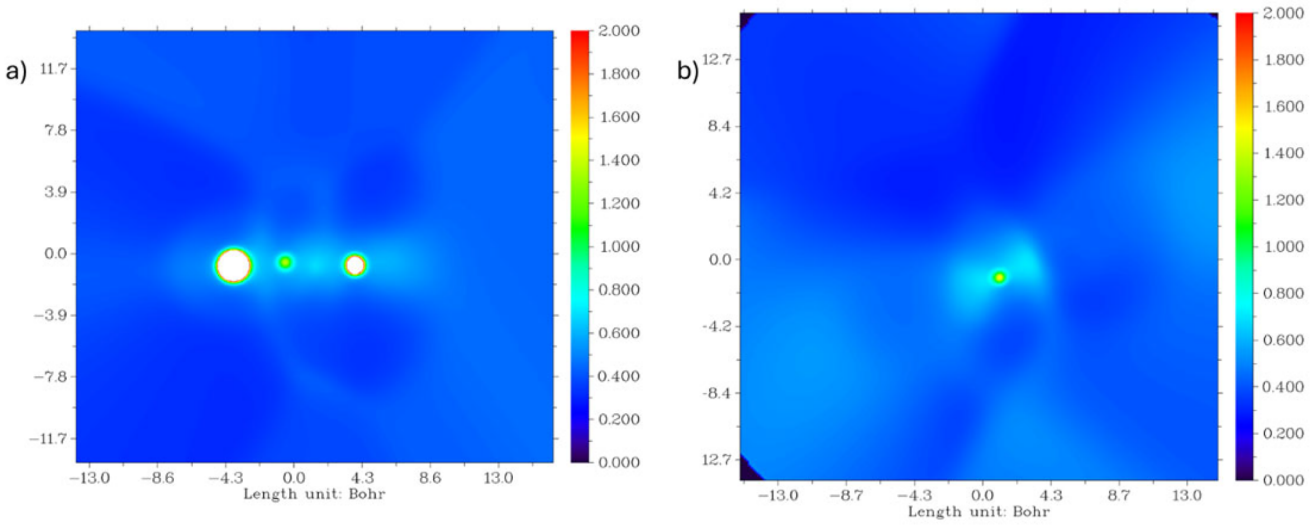

Figure 9. Average local ionization energy (ALIE) for a) m-acetamide b) 3MPAEA.

represent high confidence in predicting active toxicity (Imran et al., 2025). Thus, a probability of 0.79 for Immunotoxicity implies a strong model confidence (79%) in classifying the compound as non-immunotoxic. This underscores the importance of carefully interpreting probability scores in machine learning-based toxicity predictions, as higher numerical values can sometimes indicate a more definitive prediction of inactivity rather than an elevated risk (Di Stefano et al., 2025).

From a molecular signaling perspective, 3MPAEA showed similar inactivity across most nuclear receptor pathways and stress response pathways, with high confidence in some cases, such as the Estrogen Receptor Alpha (ER) pathway (0.87) and Aryl hydrocarbon Receptor (AhR) pathway (0.63). Regarding metabolism, the molecule demonstrated some interaction with cytochrome enzymes, particularly CYP2C19 and CYP2C9 with predictions of 0.77 and 0.74, respectively. These results indicate that while both molecules exhibit relatively low carcinogenicity and mutagenicity risks, they show potential for adverse effects on specific organs, particularly the kidneys and nervous system (Gold et al., 1993). The BBB penetration for both molecules suggests potential implications for central nervous system toxicity, which warrants further investigation (Lee et al., 2001).

3.5. Molecular docking analyses

The molecular docking analyses of m-acetamide and 3MPAEA was performed with proteins involved in ADME. Based on the protox analysis, 3MPAEA and m-acetamide were shown to interact with proteins involved in nuclear receptor signaling pathways, stress response pathways, molecular initiating events, and metabolism. The findings were observed to follow the protox analysis (Table 1 and Supplementary Material Table S7). The binding energy values were found to range between 4.3 and 6.9 kcal/mol.

3.6. Molecular dynamic analyses

In our study, we performed molecular docking and dynamic analyses with the proteins in the protox analysis. After the analysis, we determined that the molecule had higher energy (negative direction) than other proteins in docking and dynamic analyses with CYP3A4. Cytochrome P450 (CYP) 3A4, i.e., CYP3A4, oxidizes a wide range of drugs through several metabolic processes. The location of CYP3A4 in the small intestine and liver allows for effects on both presystemic and systemic drug distribution. Some interactions with CYP3A4 inhibitors may also involve inhibition of P-glycoprotein. Clinically important CYP3A4 inhibitors include itraconazole, ketoconazole, clarithromycin, erythromycin, nefazodone, ritonavir, and grapefruit juice. Usually, drug interaction varies markedly among individuals, depending on interindividual differences in CYP3A4 tissue content, preexisting medical conditions, and possibly age. Interactions may occur under single-dose conditions or only at steady state. Pharmacodynamic outcomes might closely follow pharmacokinetic changes. The clinical significance of CYP3A inhibition for drug safety and efficacy requires a closer understanding of the mechanisms for each inhibitor. Such inactivation maybe used for therapeutic gain in certain situations (Dresser et al., 2000; Zhou et al., 2005).

In the last stage of the study, molecular dynamics analysis was performed to determine the stability of the binding of molecules with proteins whose binding energy was above −6.5 kcal/mol. Fayad and colleagues performed cytotoxicity and molecular docking analysis to investigate the tubulin inhibitory activity of new acrylate-based molecules (3-(4-chlorophenyl) acrylic acids 4a,b and 3-(4-chlorophenyl) acrylate esters 5a–i). According to the obtained results, they calculated energy values of −6.7 and −6.4 kcal/mol for molecules 4b and 5e (Fayad et al., 2023). Similarly, Gören et al. (2024) calculated an energy value of −6.83 kcal/mol after the molecular docking interaction of (E)-methyl 3-(1-(4-meth oxybenzyl)-2,3-dioxoindolin-5-yl)-acrylate molecule with Fibroblast growth factor receptor 2 protein. Molecular dynamics studies analyzed the structure of AR, ARE, CAR and CYP3A4 proteins and their complexes with 3MPAEA. AR, ARE, CAR and CYP3A4 proteins were examined alone and in complexes with 3MPAEA. Figures 10–12 show the results of the AR, ARE, and CAR proteins molecular dynamics analysis, Figures 13–15 show the results of the AR, ARE, and CAR proteins complex with 3MPAEA, respectively. The CYP3A4-3MPAEA complex becomes stable in the range of 30-50 ns. In the hydrogen bond analysis, the increase in the number of bonds is associated with a decrease in the energy levels of pharmacological systems. The findings show that the average energies of the CYP3A4-3MPAEA complex are higher than the energies of the CYP3A4 protein alone, indicating that the CYP3A4-3MPAEA combination has a more effective solubilizing effect compared to the other compounds. Figures 16 and 17 summarize the molecular dynamics study presenting the determination of the binding energies of the 3MPAEA complex with CYP3A4 protein. Based on the data obtained, the 3MPAEA molecule has the potential to be a CYP3A4 inhibitor.

4. Conclusion

In this study, 2-chloro-N-(3-methoxyphenyl)acetamide (m-acetamide) and 2–(3-methoxyphenylamino)-2-oxoethyl acrylate (3MPAEA) compounds were resynthesized and characterized by Raman and UV-Visible spectroscopic techniques.

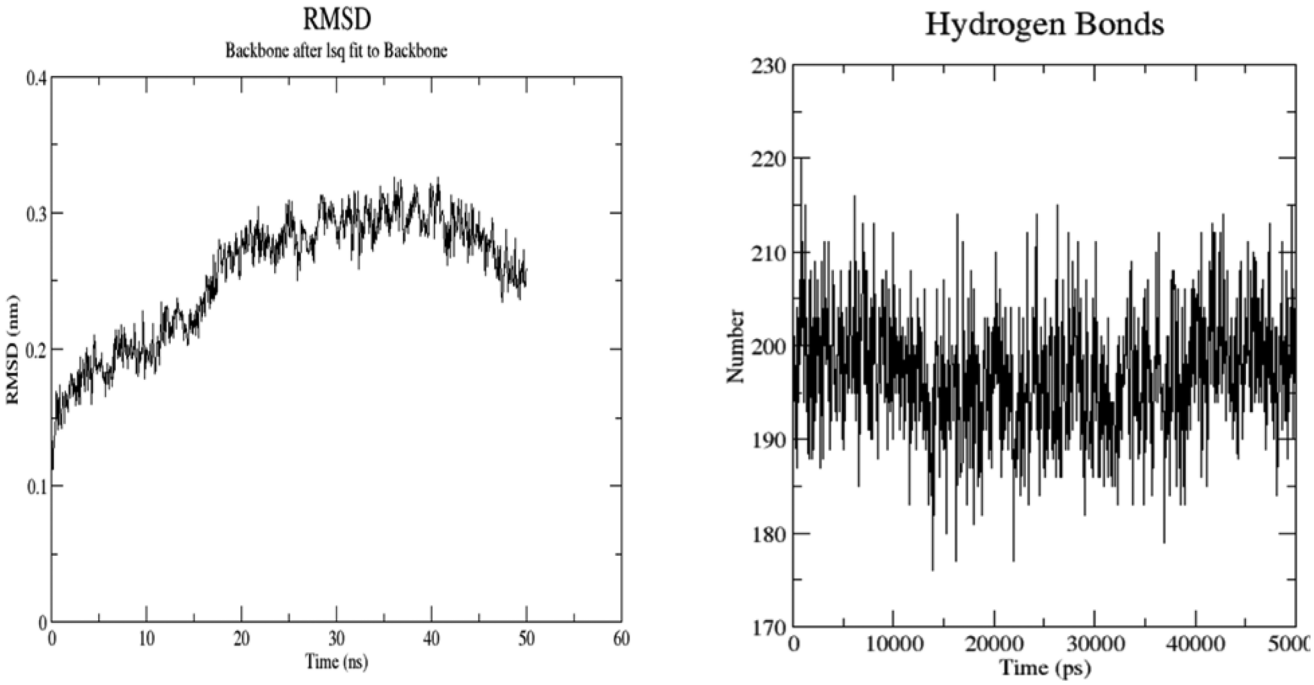

Figure 10. Molecular dynamic analyses of AR protein (RMSD and hydrogen bonds graphs).

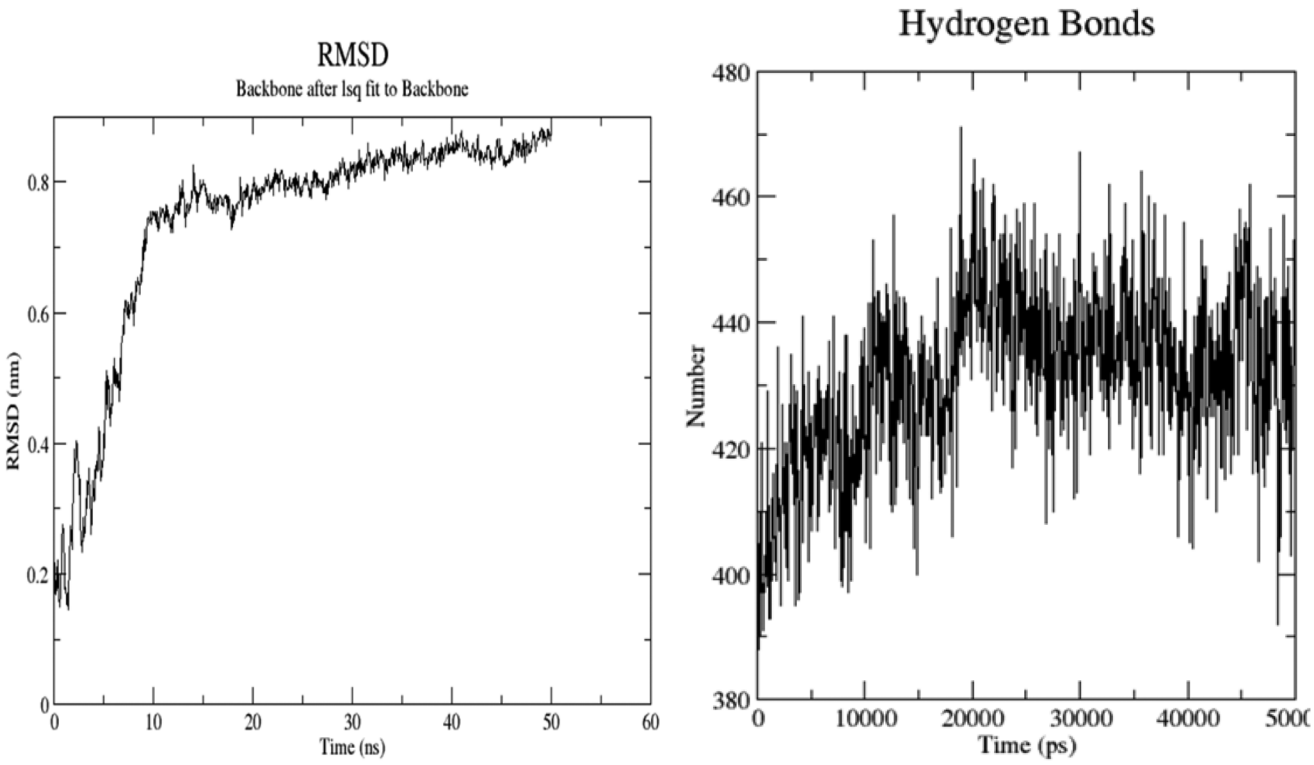

Figure 11. Molecular dynamic analyses of ARE protein (RMSD and hydrogen bonds graphs).

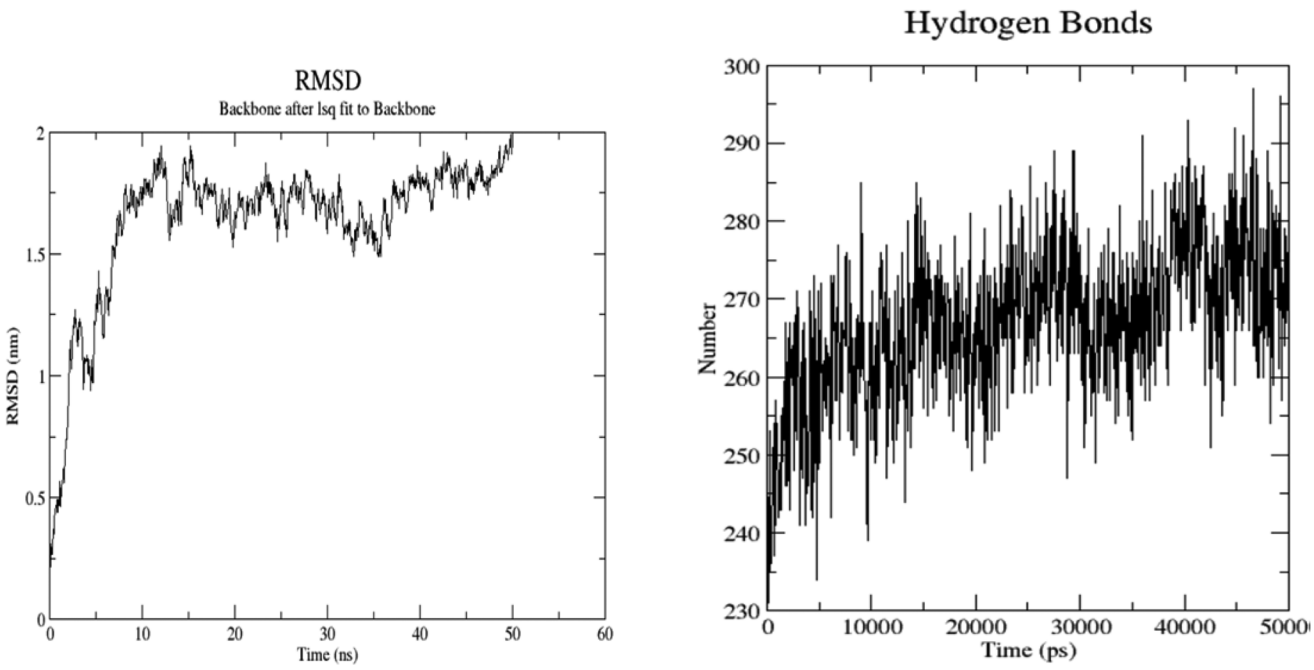

Figure 12. Molecular dynamic analyses of CAR protein (RMSD and hydrogen bonds graphs).

Optimization of geometries was performed by DFT calculations at B3LYP/6–311G and B3LYP/LanL2DZ levels, and are in good agreement with known data for similar molecules. The findings are important for understanding the photonic behavior and molecular reactivity of the compound. The Electron Localization Function (ELF) and Electrostatic Potential (ESP) analyses further are elucidated the electron distribution within the molecules, highlighting areas of electron localization and potential reactive sites. These computational analyses provided a comprehensive understanding of the electronic structure and bonding interactions in both molecules, which are crucial for their potential applications

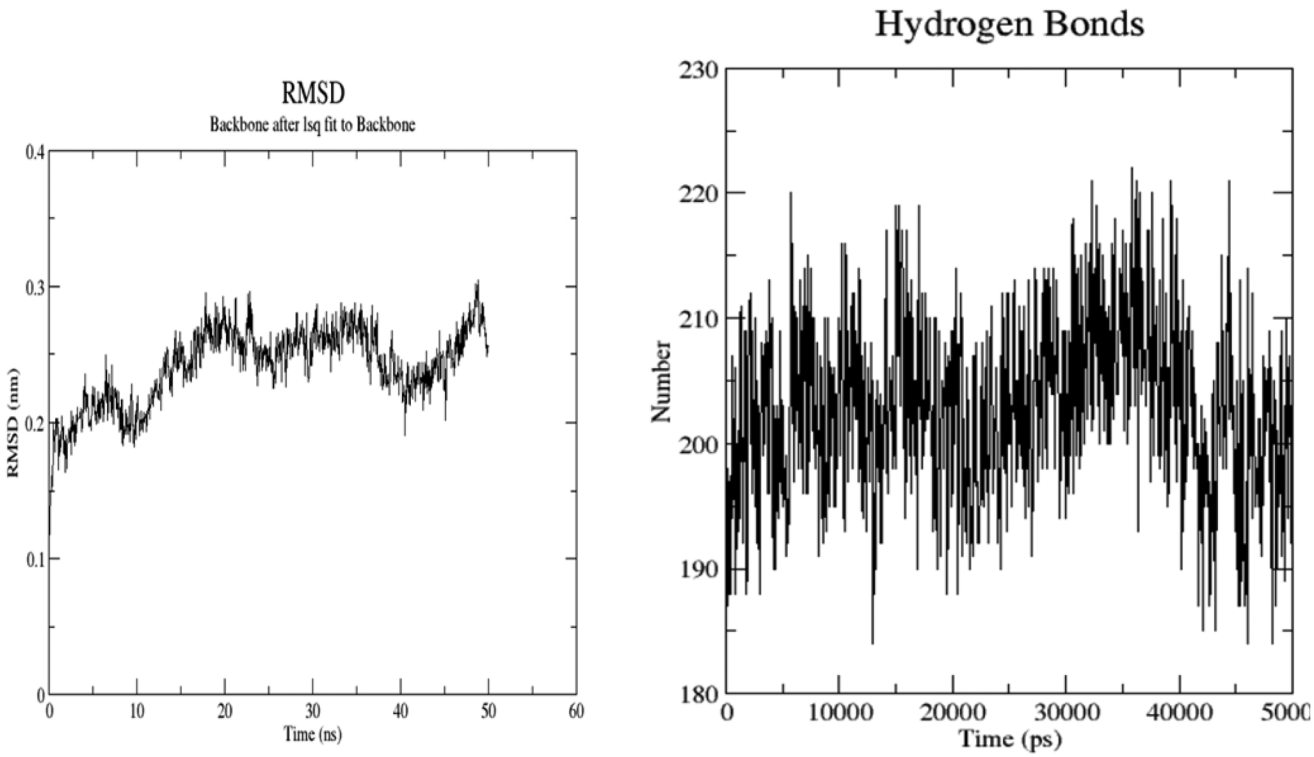

Figure 13. Molecular dynamic analyses of AR-3MPAEA complex (RMSD and hydrogen bonds graphs).

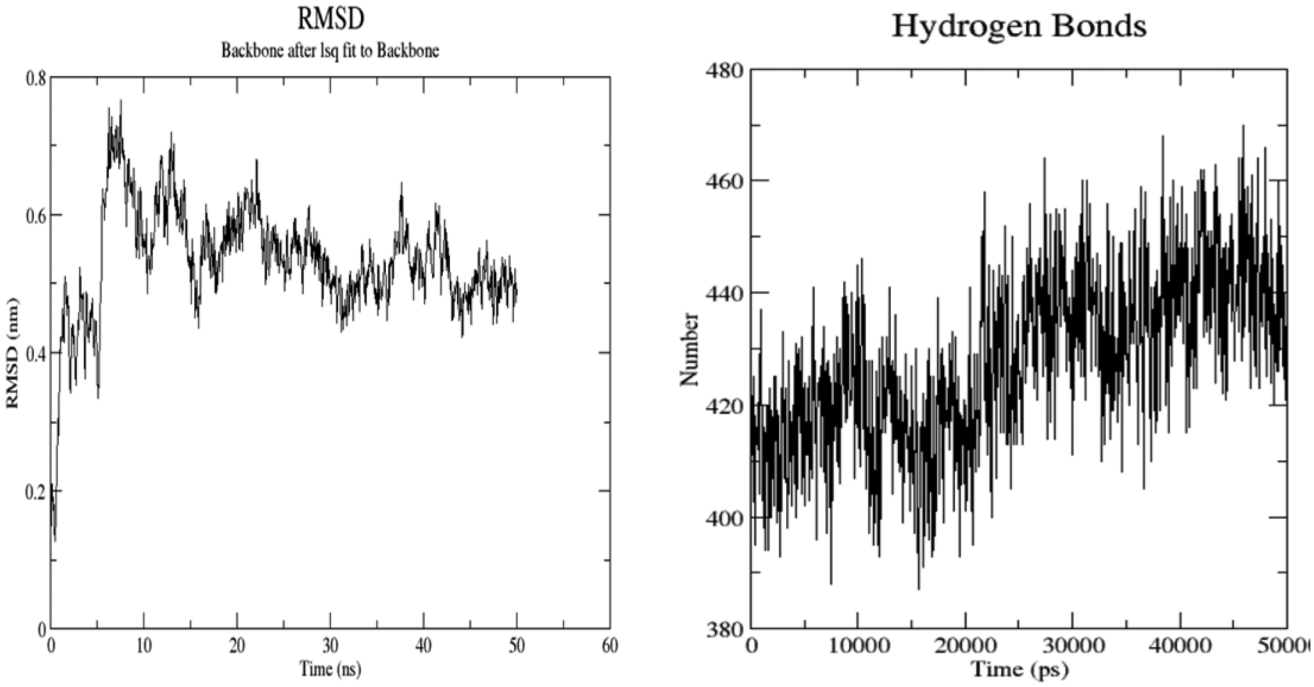

Figure 14. Molecular dynamic analyses of ARE-3MPAEA complex (RMSD and hydrogen bonds graphs).

in material science and photonic devices. In addition to structural and electronic characterization, toxicological predictions were made using the ProTox 3.0 model, which identified potential organ toxicities, including nephrotoxicity and neurotoxicity. Both m-acetamide and 3MPAEA exhibited relatively low risks for carcinogenicity and mutagenicity; however, their ability to penetrate the blood-brain barrier and impact the central nervous system necessitates further investigation. These findings provide valuable insights into the environmental and biological safety of 3MPAEA, positioning it as a promising candidate for further exploration in pharmaceutical and industrial applications. Molecular docking and dynamic analyses were also performed to investigate the interaction of 3MPAEA and m-acetamide

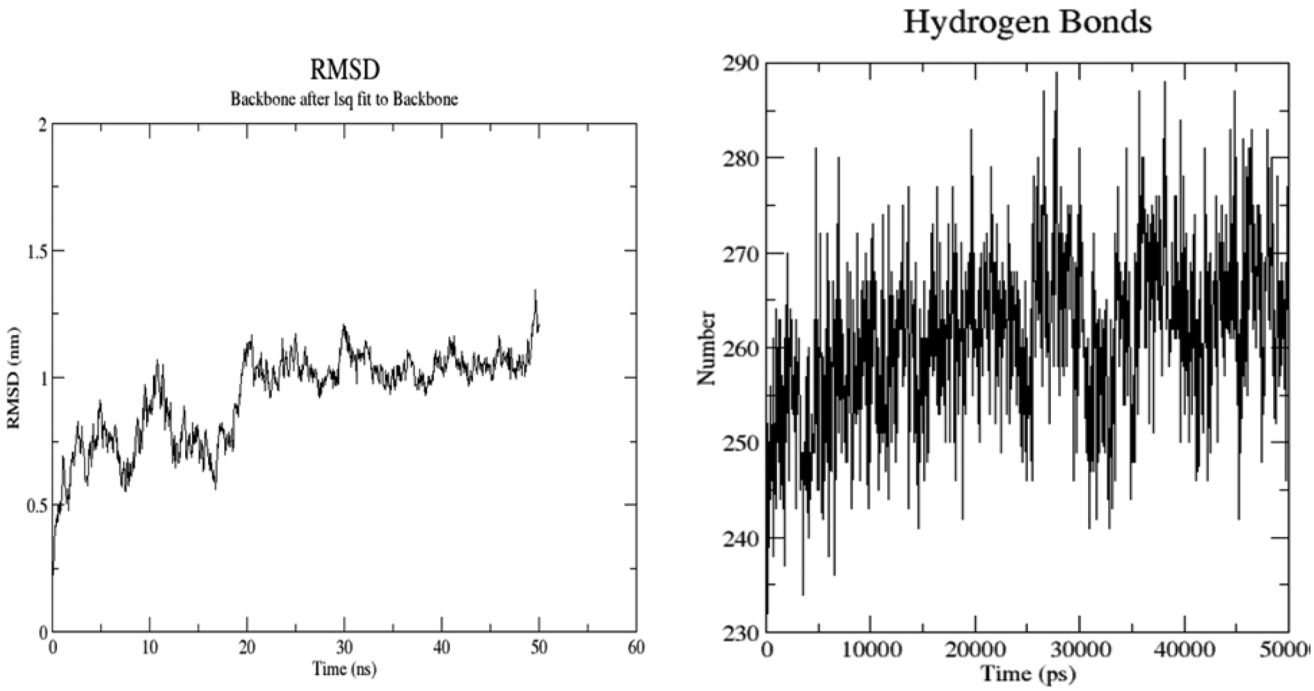

Figure 15. Molecular dynamic analyses of CAR-3MPAEA complex (RMSD and hydrogen bonds graphs).

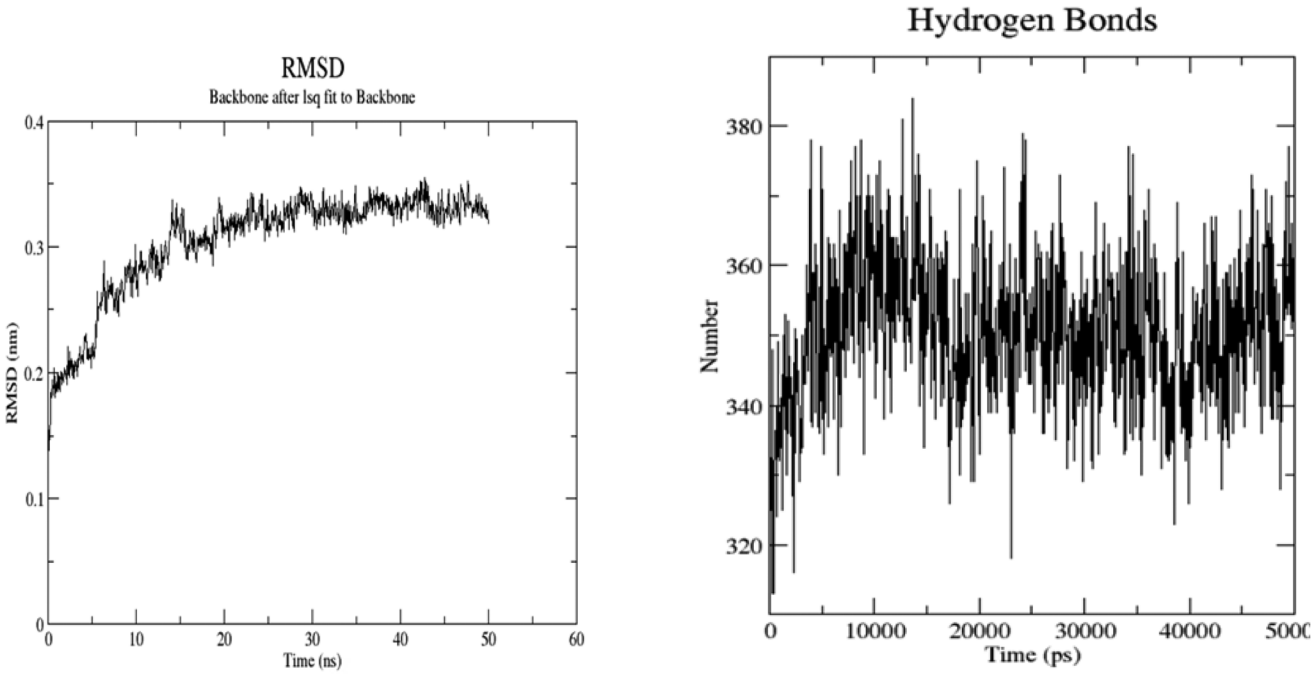

Figure 16. Molecular dynamic analyses of CYP3A4 protein (RMSD and hydrogen bonds graphs).

with proteins involved in nuclear receptor signaling, stress response pathways, molecular initiating events, and metabolism, as identified in the ProTox analysis. The results were consistent with the ProTox analysis, showing that the molecules had higher binding energies (in the negative direction) than other proteins in docking and dynamic analyses with the CYP3A4 enzyme. Cytochrome P450 (CYP) 3A4 is crucial for oxidizing a wide range of drugs through various metabolic processes, and its location in the small intestine and liver affects both presystemic and systemic drug distribution. Some interactions with CYP3A4 inhibitors may also inhibit P-glycoprotein. This highlights the importance of understanding drug interactions, as variations in CYP3A4 content and individual differences can influence pharmacodynamic and pharmacokinetic outcomes. This study introduces 3MPAEA as a novel acrylate derivative with significant potential for drug development and material science applications. It also provides an in-depth understanding of its

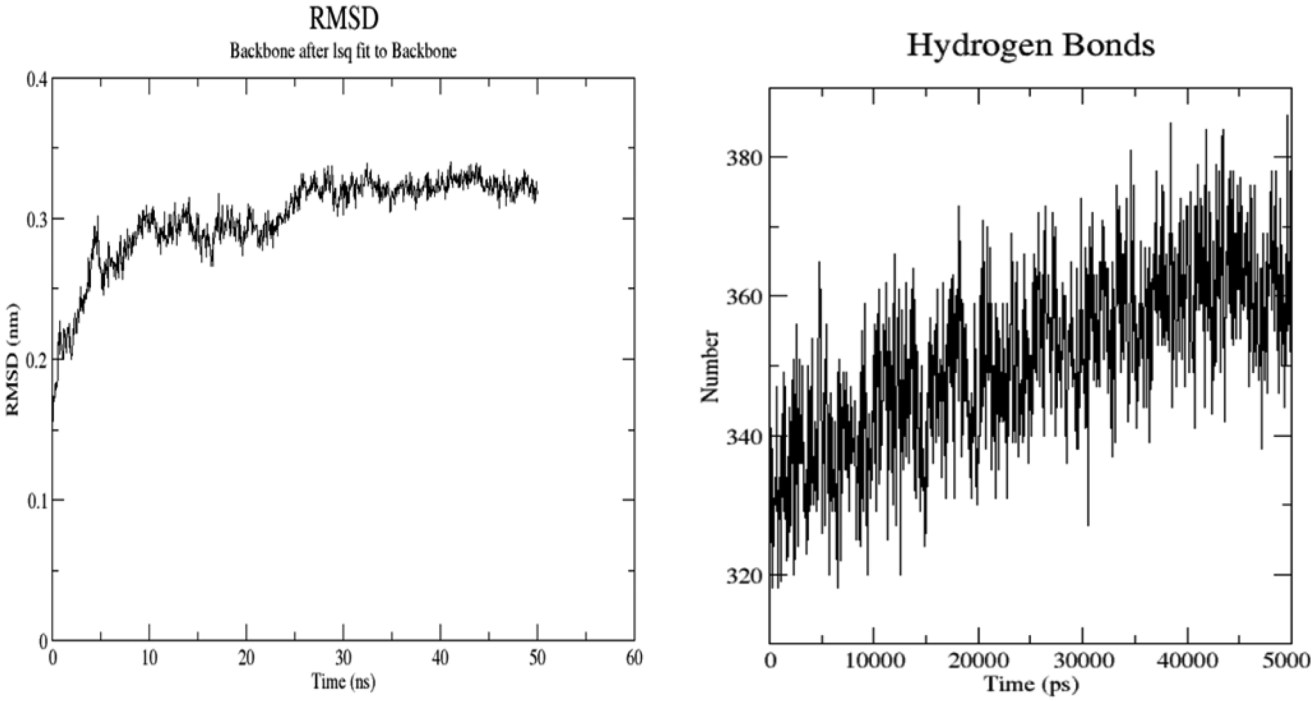

Figure 17. Molecular dynamic analyses of CYP3A4-3MPAEA complex (RMSD and hydrogen bonds graphs).

electronic and toxicological properties. Future studies should focus on experimentally validating the predicted toxicological risks and exploring the compound's functional applications in advanced material design and biomedical research.

Disclosure statement

No potential conflict of interest was reported by the author(s).

Ethical statement

This study did not include any humans or animals; therefore, we did not apply for ethical approval or register for clinical trials.

Author contributions

These authors have made equal contributions.

Funding

The author(s) reported there is no funding associated with the work featured in this article.

ORCID

Nevin Çankaya http://orcid.org/0000-0002-6079-4987
Mehmet Hanifi Kebiroğlu http://orcid.org/0000-0002-6764-3364
Serap Yalcin Azarkan http://orcid.org/0000-0002-9584-266X

Data availability statement

Data is within the manuscript. The data underlying this article will be shared on reasonable request to the corresponding author.

References

Abdelaziz, B., Mazouz, Z., Gassoumi, B., Boukortt, N. E. I., Patanè, S., & Ayachi, S. (2024). Molecular engineering of D-π-A-type structures based on nitrobenzofurazan (NBD) derivatives for both organic solar cells and nonlinear optical response. *Journal of Molecular Liquids*, *395*, 123934. https://doi.org/10.1016/j.molliq.2023.123934

Abraham, M. J., Murtola, T., Schulz, R., Páll, S., Smith, J. C., Hess, B., & Lindahl, E. (2015). GROMACS: High performance molecular simulations through multi-level parallelism from laptops to supercomputers. *SoftwareX*, *1-2*, 19–25. https://doi.org/10.1016/j.softx.2015.06.001

Ak, F., & Kebiroglu, M. H. (2024). Theoretical investigation of the chemical reactivity of acrylic acid molecules: A DFT study with UV-Vis, NMR, and FT-IR spectroscopy using STO-3G basis set. *Yüzüncü Yıl Üniversitesi Fen Bilimleri Enstitüsü Dergisi*, *29*(2), 438–446. https://doi.org/10.53433/yyufbed.1350755

Akman, F. (2025). Research on the molecular structure, solvent effects, quantum computing, topology, and biological aspects of 4-phenylcoumarin-7-yl-methacrylate as an anticancer agent. *Journal of Molecular Structure*, *1320*, 139660. https://doi.org/10.1016/j.molstruc.2024.139660

Akman, F., Demirpolat, A., Kazachenko, A. S., Kazachenko, A. S., Issaoui, N., & Al-Dossary, O. (2023). Molecular structure, electronic properties, reactivity (ELF, LOL, and Fukui), and NCI-RDG studies of the binary mixture of water and essential oil of Phlomis bruguieri. *Molecules (Basel, Switzerland)*, *28*(6), 2684. https://doi.org/10.3390/molecules28062684

Alhewaitey, A. M., Khan, I., & Buabeng, E. R. (2024). Advancements in polymer science: Synthesis, characterization, and biomedical applications of homopolymers and copolymers. *Open Journal of Polymer Chemistry*, *14*(3), 167–198. https://doi.org/10.4236/ojpchem.2024.143008

Arulaabaranam, K., Muthu, S., Mani, G., & Irfan, A. (2021). Conformational study, FT-IR, FT-Raman, solvent effect on UV–Vis, charge transfer and protein–ligand interactions of Methyl-2-pyrazinecarboxylate. *Journal of Molecular Liquids*, *341*, 116934. https://doi.org/10.1016/j.molliq.2021.116934

Azzouzi, M., Azougagh, O., Ouchaoui, A. A., El Hadad, S. E., Mazières, S., Barkany, S. E., Abboud, M., & Oussaid, A. (2024). Synthesis, characterizations, and quantum chemical investigations on imidazo [1, 2-a] pyrimidine-Schiff base derivative:(E)-2-Phenyl-N-(thiophen-2-ylmethy-

lene) imidazo [1, 2-a] pyrimidin-3-amine. *ACS Omega*, *9*(1), 837–857. https://doi.org/10.1021/acsomega.3c06841

Banerjee, P., Kemmler, E., Dunkel, M., & Preissner, R. (2024). ProTox 3.0: a webserver for the prediction of toxicity of chemicals. *Nucleic Acids Research*, *52*(W1), W513–W520. https://doi.org/10.1093/nar/gkae303

Bjelkmar, P., Larsson, P., Cuendet, M. A., Hess, B., & Lindahl, E. (2010). Implementation of the CHARMM force field in GROMACS: analysis of protein stability effects from correction maps, virtual interaction sites, and water models. *Journal of Chemical Theory and Computation*, *6*(2), 459–466. https://doi.org/10.1021/ct900549r

Boehmke Amoruso, A., Boto, R. A., Elliot, E., de Nijs, B., Esteban, R., Földes, T., Aguilar-Galindo, F., Rosta, E., Aizpurua, J., & Baumberg, J. J. (2024). Uncovering low-frequency vibrations in surface-enhanced Raman of organic molecules. *Nature Communications*, *15*(1), 6733. https://doi.org/10.1038/s41467-024-50823-x

Boittier, E., Töpfer, K., Devereux, M., & Meuwly, M. (2024). Kernel-based minimal distributed charges: A conformationally dependent ESP-model for molecular simulations. *Journal of Chemical Theory and Computation*, *20*(18), 8088–8099. https://doi.org/10.1021/acs.jctc.4c00759

Çankaya, N., Kebiroğlu, M. H., & Temüz, M. M. (2024). A comprehensive study of experimental and theoretical characterization and in silico toxicity analysis of new molecules. *Drug and Chemical Toxicology*, *47*(6), 1226–1240. https://doi.org/10.1080/01480545.2024.2353724

Çoban, V., Çankaya, N., & Azarkan, S. Y. (2024). New oxomethacrylate and acetamide: synthesis, characterization, and their computational approaches: molecular docking, molecular dynamics, and ADME analyses. *Drug and Chemical Toxicology*, *47*(6), 1175–1184. https://doi.org/10.1080/01480545.2024.2349651

Di Stefano, M., Piazza, L., Poles, C., Galati, S., Granchi, C., Giordano, A., Campisi, L., Macchia, M., Poli, G., & Tuccinardi, T. (2025). KinasePred: A computational tool for small-molecule kinase target prediction. *International Journal of Molecular Sciences*, *26*(5), 2157. https://doi.org/10.3390/ijms26052157

Dresser, G. K., Spence, J. D., & Bailey, D. G. (2000). Pharmacokinetic-pharmacodynamic consequences and clinical relevance of cytochrome P450 3A4 inhibition. *Clinical Pharmacokinetics*, *38*(1), 41–57. https://doi.org/10.2165/00003088-200038010-00003

Drwal, M. N., Banerjee, P., Dunkel, M., Wettig, M. R., & Preissner, R. (2014). ProTox: a web server for the in silico prediction of rodent oral toxicity. *Nucleic Acids Research*, *42*(Web Server issue), W53–W58. https://doi.org/10.1093/nar/gku401

Fayad, E., Altalhi, S. A., Abualnaja, M. M., Alrohaimi, A. H., Elsaid, F. G., Abu Almaaty, A. H., Saleem, R. M., Bazuhair, M. A., Ahmed Maghrabi, A. H., Beshay, B. Y., & Zaki, I. (2023). Novel acrylate-based derivatives: Design, synthesis, antiproliferative screening, and docking study as potential combretastatin analogues. *ACS Omega*, *8*(41), 38394–38405. https://doi.org/10.1021/acsomega.3c05051

GP, S. M., Aruldhas, D., Hubert Joe, I., Selvaraj, S., G. Nadh, A., & Kunhikrishnan, J. (2024). Quantum chemical investigations, Hirschfeld surface analysis, FMO, MESP, topology analyses, in-silico analysis and pharmacokinetics properties of 3-chloro-N-(4-hydroxy-3-methoxy-benzyl)-2, 2-dimethyl propanamide [CHMBDP]. *Molecular Crystals and Liquid Crystals*, *768*(18), 1146–1162. https://doi.org/10.1080/15421406.2024.2381292

Gatfaoui, S., Issaoui, N., Brandán, S. A., Medimagh, M., Al-Dossary, O., Roisnel, T., Marouani, H., & Kazachenko, A. S. (2022). Deciphering non-covalent interactions of 1, 3-Benzenedimethanaminium bis (trioxonitrate): Synthesis, empirical and computational study. *Journal of Molecular Structure*, *1250*, 131720. https://doi.org/10.1016/j.molstruc.2021.131720

Gatfaoui, S., Issaoui, N., Roisnel, T., & Marouani, H. (2019). A proton transfer compound template phenylethylamine: synthesis, a collective experimental and theoretical investigations. *Journal of Molecular Structure*, *1191*, 183–196. https://doi.org/10.1016/j.molstruc.2019.04.093

Ghalla, H., Issaoui, N., Govindarajan, M., Flakus, H. T., Jamroz, M. H., & Oujia, B. (2014). Spectroscopic and molecular structure investigation of 2-furanacrylic acid monomer and dimer using HF and DFT methods. *Journal of Molecular Structure*, *1059*, 132–143. https://doi.org/10.1016/j.molstruc.2013.11.037

Gold, L. S., Slone, T. H., Stern, B. R., & Bernstein, L. (1993). Comparison of target organs of carcinogenicity for mutagenic and non-mutagenic chemicals. *Mutation Research*, *286*(1), 75–100. https://doi.org/10.1016/0027-5107(93)90004-y

Gören, K., Bağlan, M., & Yıldıko, Ü. (2024). Melanoma cancer evaluation with ADME and molecular docking analysis, DFT calculations of (E)-methyl 3-(1-(4-methoxybenzyl)-2, 3-dioxoindolin-5-yl)-acrylate molecule. *Iğdır Üniversitesi Fen Bilimleri Enstitüsü Dergisi*, *14*(3), 1186–1199. https://doi.org/10.21597/jist.1467666

Habiballah, S., Heath, L. S., & Reisfeld, B. (2024). A deep-learning approach for identifying prospective chemical hazards. *Toxicology*, *501*, 153708. https://doi.org/10.1016/j.tox.2023.153708

Halim, S. A., El-Meligy, A. B., El-Nahas, A. M., & El-Demerdash, S. H. (2024). DFT study, and natural bond orbital (NBO) population analysis of 2-(2-Hydroxyphenyl)-1-azaazulene tautomers and their mercapto analouges. *Scientific Reports*, *14*(1), 219. https://doi.org/10.1038/s41598-023-50660-w

Hyun, Y., & Kim, D. (2024). Artificial intelligence-empowered spectroscopic single molecule localization microscopy. *Small Methods*, e2401654. https://doi.org/10.1002/smtd.202401654

Imran, M. M., Zita, R., Copeland, R., Chatterjee, P., Rahman, R. R., & Damevski, K. (2025). Understanding and predicting derailment in toxic conversations on GitHub. *arXiv:2503.02191*. https://doi.org/10.48550/arXiv.2503.02191

Joseph, D., Alharbi, N. S., Abbas, G., & Sambantham, M. (2024). Vibrational spectra, effect of solvents in UV-visible, electronic properties, charge distribution, molecular interaction and Fukui analysis on 3-amino-2, 5-dichloropyridine. *Zeitschrift Für Physikalische Chemie*, *238*(4), 661–681. https://doi.org/10.1515/zpch-2023-0462

Jurowski, K., & Krośniak, A. (2024). Prediction of key toxicity endpoints of AP-238 a new psychoactive substance for clinical toxicology and forensic purposes using in silico methods. *Scientific Reports*, *14*(1), 28977. https://doi.org/10.1038/s41598-024-79453-5

Jurowski, K., Niżnik, Ł., Frydrych, A., Kobylarz, D., Noga, M., Krośniak, A., Fijałkowska, O., Świdniak, A., & Ahuja, V. (2025). Toxicological profile of Acovenoside A as an active pharmaceutical ingredient–prediction of missing key toxicological endpoints using in silico toxicology methodology. *Chemico-Biological Interactions*, *408*, 111404. https://doi.org/10.1016/j.cbi.2025.111404

Kurban, M., Sertbakan, T. R., & Muz, İ. (2024). Computational analysis and experimental validation of a quinoline derivative for optoelectronic and pharmacological applications. *Materials Today Communications*, *39*, 108642. https://doi.org/10.1016/j.mtcomm.2024.108642

Lee, G., Dallas, S., Hong, M., & Bendayan, R. (2001). Drug transporters in the central nervous system: brain barriers and brain parenchyma considerations. *Pharmacological Reviews*, *53*(4), 569–596. https://doi.org/10.1016/S0031-6997(24)01513-8

Lindorff-Larsen, K., Piana, S., Palmo, K., Maragakis, P., Klepeis, J. L., Dror, R. O., & Shaw, D. E. (2010). Improved side-chain torsion potentials for the Amber ff99SB protein force field. *Proteins*, *78*(8), 1950–1958. https://doi.org/10.1002/prot.22711

Manogaran, K., Sivaranjani, T., Sengeny, P., Venkatachalapathy, V. S. K., Mahadevan, M., Elangovan, K., Armaković, S., Armaković, S. J., & Abramović, B. F. (2024). Investigation on molecular and biomolecular spectroscopy of the novel 2BCA molecule to analyse its biological activities and binding interaction with nipah viral protein. *Spectrochimica Acta. Part A, Molecular and Biomolecular Spectroscopy*, *321*, 124737. https://doi.org/10.1016/j.saa.2024.124737

Medimagh, M., Issaoui, N., Gatfaoui, S., Brandán, S. A., Al-Dossary, O., Marouani, H., & Wojcik, M. J. (2021). Impact of non-covalent interactions on FT-IR spectrum and properties of 4-methylbenzylammonium nitrate. A DFT and molecular docking study. *Heliyon*, *7*(10), e08204. https://doi.org/10.1016/j.heliyon.2021.e08204

Murail, S., De Vries, S. J., Rey, J., Moroy, G., & Tufféry, P. (2021). SeamDock: an interactive and collaborative online docking resource to assist small compound molecular docking. *Frontiers in Molecular Biosciences*, *8*, 716466. https://doi.org/10.3389/fmolb.2021.716466

Nikrou Siahsary, M. R., Ebrahimi, A., & Habibi Khorasani, M. (2024). A systematic study on interplay between intermolecular hydrogen bonding and aromaticity. *Molecular Physics*, *122*(14), e2302384. https://doi.org/10.1080/00268976.2024.2302384

Obloy, L. M., Jockusch, S., & Tarnovsky, A. N. (2024). Shortwave infrared polymethine dyes for bioimaging: ultrafast relaxation dynamics and excited-state decay pathways. *Physical Chemistry Chemical Physics: PCCP*, *26*(37), 24261–24278. https://doi.org/10.1039/d4cp01411a

Oostenbrink, C., Villa, A., Mark, A. E., & Van Gunsteren, W. F. (2004). A biomolecular force field based on the free enthalpy of hydration and solvation: the GROMOS force-field parameter sets 53A5 and 53A6. *Journal of Computational Chemistry*, *25*(13), 1656–1676. https://doi.org/10.1002/jcc.20090

Patil, V. M., Gupta, S. P., Masand, N., & Balasubramanian, K. (2024). Experimental and computational models to understand protein-ligand, metal-ligand and metal-DNA interactions pertinent to targeted cancer and other therapies. *European Journal of Medicinal Chemistry Reports*, *10*, 100133. https://doi.org/10.1016/j.ejmcr.2024.100133

Qiao, T., Shi, W., Zhuang, H., Zhao, G., Xin, X., & Li, Y. (2024). Effects of substitution and conjugation on photophysical properties of ESIPT-based fluorophores with the core of 4-aminophthalimide. *Spectrochimica Acta. Part A, Molecular and Biomolecular Spectroscopy*, *309*, 123802. https://doi.org/10.1016/j.saa.2023.123802

Ramalingam, A., Kuppusamy, M., Sambandam, S., Medimagh, M., Oyeneyin, O. E., Shanmugasundaram, A., Issaoui, N., & Ojo, N. D. (2022). Synthesis, spectroscopic, topological, hirshfeld surface analysis, and anti-covid-19 molecular docking investigation of isopropyl 1-benzoyl-4-(benzoyloxy)-2, 6-diphenyl-1, 2, 5, 6-tetrahydropyridine-3-carboxylate. *Heliyon*, *8*(10), e10831. https://doi.org/10.1016/j.heliyon.2022.e10831

Reeda, V. J., Sakthivel, S., Divya, P., Javed, S., & Jothy, V. B. (2024). Conformational stability, quantum computational (DFT), vibrational, electronic and non-covalent interactions (QTAIM, RDG and IGM) of antibacterial compound N-(1-naphthyl) ethylenediamine dihydrochloride. *Journal of Molecular Structure*, *1298*, 137043. https://doi.org/10.1016/j.molstruc.2023.137043

Rifa, R. A., Rojo, M. G., & Lavado, R. (2025). Mechanisms of toxicity caused by bisphenol analogs in human in vitro cell models. *Chemico-Biological Interactions*, *412*, 111475. https://doi.org/10.1016/j.cbi.2025.111475

Salah, T., Mhadhbi, N., Ben Ahmed, A., Hamdi, B., Krayem, N., Loukil, M., Guesmi, A., Khezami, L., Houas, A., Ben Hamadi, N., Naïli, H., & Costantino, F. (2023). Physico-chemical characterization, DFT modeling and biological activities of a new Zn (II) complex containing melamine as a template. *Crystals*, *13*(5), 746. https://doi.org/10.3390/cryst13050746

Smati, S., Djafri, A., Menad, K., Boukabcha, N., Rahmani, R., Goudjil, M., Megrouss, Y., Khaldi, H., Dege, N., Chouaih, A., & Djafri, A. (2024). Synthesis, molecular structure, Hirshfeld surface analysis, NCI-RDG, spectral characterization analysis, nonlinear optical properties, and in silico molecular docking of (E)-3-(3-(2-methoxyphenyl)-4-methylth iazol-2 (3H)-ylidene) benzo [4, 5] imidazo [1, 2-c] thiazole-1 (3H)-thione. *Journal of Molecular Structure*, *1318*, 139157. https://doi.org/10.1016/j.molstruc.2024.139157

Sturla, S. J., Boobis, A. R., FitzGerald, R. E., Hoeng, J., Kavlock, R. J., Schirmer, K., Whelan, M., Wilks, M. F., & Peitsch, M. C. (2014). Systems toxicology: from basic research to risk assessment. *Chemical Research in Toxicology*, *27*(3), 314–329. https://doi.org/10.1021/tx400410s

Trott, O., & Olson, A. J. (2010). AutoDock Vina: improving the speed and accuracy of docking with a new scoring function, efficient optimization, and multithreading. *Journal of Computational Chemistry*, *31*(2), 455–461. https://doi.org/10.1002/jcc.21334

Vidal, L., Barrena-Espés, D., Echeverría, J., Munárriz, J., & Pendás, Á. M. (2024). Deciphering pyramidanes: A quantum chemical topology approach. *Chemphyschem: a European Journal of Chemical Physics and Physical Chemistry*, *25*(22), e202400329. https://doi.org/10.1002/cphc.202400329

Xiong, Z., Zhang, J., Zhang, Z., Wang, L., Wei, S., Liu, X., Sun, J. Z., Zhang, H., & Tang, B. Z. (2024). Activating electronic delocalization: Through-space lone-pair interactions versus hydrogen bonding. *ACS Materials Letters*, *6*(9), 3941–3950. https://doi.org/10.1021/acsmaterialslett.4c01182

Yadav, D., Giri, P., & Das, C. (2024). Polymer-based biomaterials and their applications in tissue adhesives. *Journal of Adhesion Science and Technology*, *38*(12), 2019–2046. https://doi.org/10.1080/01694243.2023.2288424

Yalçınkaya, S., Azarkan, S. Y., & Çakmakçı, A. G. K. (2022). Determination of the effect of L. plantarum AB6-25, L. plantarum MK55 and S. boulardii T8-3C microorganisms on colon, cervix, and breast cancer cell lines: Molecular docking, and molecular dynamics study. *Journal of Molecular Structure*, *1261*, 132939. https://doi.org/10.1016/j.molstruc.2022.132939

Ylivainio, K. J. (2024). Exploring the correlation between electron localization function and binding energy in bimolecular systems. https://www.diva-portal.org/smash/record.jsf?pid=diva2:1876667

Zhang, S., Makoś, M. Z., Jadrich, R. B., Kraka, E., Barros, K., Nebgen, B. T., Tretiak, S., Isayev, O., Lubbers, N., Messerly, R. A., & Smith, J. S. (2024). Exploring the frontiers of condensed-phase chemistry with a general reactive machine learning potential. *Nature Chemistry*, *16*(5), 727–734. https://doi.org/10.1038/s41557-023-01427-3

Zhao, P., Li, T., Wei, D., Wu, D., Wang, L., & Duan, Z. (2024). Synthesis, photophysical and electrochemical properties of spiro-phosphonium compounds. *The Journal of Organic Chemistry*, *89*(16), 11109–11118. https://doi.org/10.1021/acs.joc.3c02651

Zhou, J., Bie, J., Wang, X., Liu, Q., Li, R., Chen, H., Hu, J., Cao, H., Ji, W., Li, Y., Liu, S., Shen, Z., & Xu, B. (2020). Discovery of n-arylsulfonyl-indole-2-carboxamide derivatives as potent, selective, and orally bioavailable fructose-1, 6-bisphosphatase inhibitors—design, synthesis, in vivo glucose lowering effects, and x-ray crystal complex analysis. *Journal of Medicinal Chemistry*, *63*(18), 10307–10329. https://doi.org/10.1021/acs.jmedchem.0c00726

Zhou, S., Chan, S. Y., Goh, B. C., Chan, E., Duan, W., Huang, M., & McLeod, H. L. (2005). Mechanism-based inhibition of cytochrome P450 3A4 by therapeutic drugs. *Clinical Pharmacokinetics*, *44*(3), 279–304. https://doi.org/10.2165/00003088-200544030-00005

Zucolotto Cocca, L. H., Valverde, J. V. P., Le Bescont, J., Breton-Patient, C., Piguel, S., Silva, D. L., Mendonca, C. R., & De Boni, L. (2024). Photophysical properties of 3-arylthioimidazo [1, 2-a] pyridine derivatives: The role of peripheral electron-donating and electron-withdrawing groups in the advance of organic materials engineering. *Journal of Molecular Structure*, *1300*, 137221. https://doi.org/10.1016/j.molstruc.2023.137221